JOURNAL OF MATERIALS SCIENCE 27 (1992) 2423–2428

Tensile behaviour of borosilicate glass matrix–Nicalon (silicon carbide) fibre composites

V. RAMAKRISHNAN, N. JAYARAMAN
Department of Materials Science and Engineering, University of Cincinnati, Cincinnati, OH 45221, USA

Unidirectional composites consisting of a borosilicate glass (Corning 7740) matrix reinforced with Nicalon (silicon carbide) fibres were fabricated and tested in monotonic tension at temperatures ranging from room temperature to 650 °C. The ultimate tensile strength showed little dependence on temperature up to about 425 °C and failed by longitudinal splitting. There was a significant increase in strength at 540 °C and a slight decrease in strength when tested above this temperature, and the failure involved extensive fibre pull-out. The elastic modulus (stiffness) was found to decrease progressively with increasing temperature. The matrix consists of borosilicate glass within the plies and very fine grains of alpha (low) cristobalite in the inter-ply regions. The behaviour of the composite as a whole was found to be dependent upon the behaviour of the matrix at the temperature of testing.

1. Introduction

Glass-ceramic matrices reinforced with ceramic fibres provide great potential for high-temperature use and are an active expanding field of development. They have been found to possess high strength, high stiffness, excellent toughness and low density [1, 2].

While initial studies [3, 4] depended heavily on three- and four-point bend tests for mechanical property characterization, much progress has been made [5] towards developing methods for reliably testing these materials in monotonic tension. Two glass matrices that have been studied extensively are lithium–aluminium–silicate (LAS) glass and borosilicate glass. LAS glasses generally have higher service temperature capabilities and exhibit higher strength levels.

Borosilicate glass matrices reinforced with Nicalon silicon carbide-type yarn provide a model system to study the mechanical behaviour of glass and ceramic matrix composites mainly due to the high degree of compatibility between the fibre and the matrix. The coefficient of thermal expansion [1, 2] for borosilicate glass is $3.25 \times 10^{-6}\,°C^{-1}$ and that for Nicalon fibres is $4.0 \times 10^{-6}\,°C^{-1}$. The fact that these values are so close to each other gives rise to lower residual stresses on fabrication. Another attractive feature of these composites is the relative ease in processing of the composite. The manufacturing process [6, 7] is simplified mainly due to the unique capability of glasses to be densified in the glassy state and then crystallized by controlling the processing temperatures. The availability of silicon carbide fibres in the form of a yarn, i.e. Nicalon, makes it easier to incorporate it as a reinforcement in the composite.

This paper describes the mechanical properties and failure mechanisms of a glass-ceramic composite of borosilicate matrix reinforced with Nicalon fibres up to 650 °C.

2. Composite fabrication

The basic process used for the manufacture of these composites was developed at the United Technologies Research Center by Prewo *et al.* [1]. The procedure followed at the University of Cincinnati consisted of three stages. The first stage consisted of passing the filaments through a slurry containing glass frit (325 mesh) with a binder (Robond) and winding it on a hexagonal drum. After drying, these pre-pregs were stacked to give eight unidirectional plies and the binder was burned out by heating the plies to 500 °C for 30 min. The final stage in the manufacture was hot pressing which was done at 1000 °C, the sample being held under a pressure of 1000 p.s.i. (10^3 p.s.i. = 6.89 $N\,mm^{-2}$) for 15 min in a graphite die using graphite punches. This was followed by furnace cooling in argon and under pressure. The pressure was removed once the softening point (821 °C) was passed.

3. Composite characterization

X-ray diffraction was performed on the as-fabricated samples as well as samples heat treated at 540 and 650 °C. The heat-treatment procedure was as follows. The sample was heated and held at temperature for 30 min and then quenched in water. The diffraction peaks observed in all cases were found to be those of alpha (low) cristobalite polymorph of SiO_2.

0022–2461

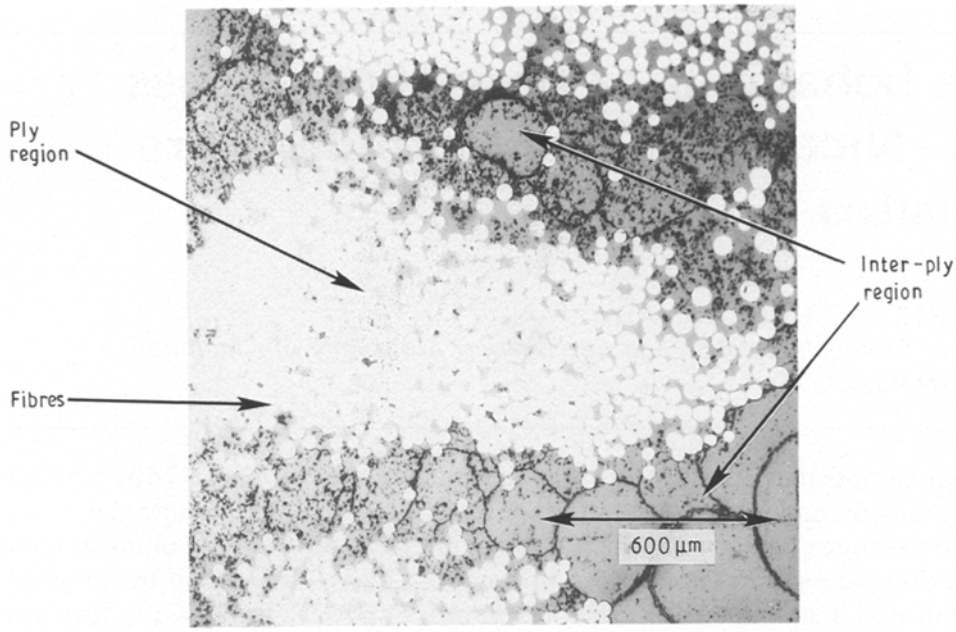

Figure 1 Microstructure of as-fabricated composite showing the ply and interply regions.

The microstructure of the as-fabricated sample (Fig. 1) shows two distinct regions within the composite, namely the ply region consisting of both fibres and matrix, and the interply regions consisting of matrix alone. Notwithstanding the distribution, the volume fraction of fibres was calculated to be around 0.35 from similar photomicrographs. This volume fraction does not include the glass in the interply region. Fig. 2 reveals that the structure of the matrix material in the ply regions and interply regions is quite different. This photograph was taken after etching an as-fabricated sample in 1% HF. The matrix material around the fibres within the ply regions appears to be fully glass. The interply regions, on the other hand, reveal an almost fully crystalline structure with very fine silica crystals. There are also thick grain-boundary-like features in the interply region which appear to be fully glass. The fact that this phase is glassy is borne out by the fact that it is etched by 20% HCl which will etch away most glasses but leave the alpha cristobalite untouched [8, 9]. These features are shown in micrographs in Fig. 2 and schematically in Fig. 3.

The glassy phase in the interply "grain-boundary" region seems to be darker than the ply region glass in Fig. 2. An educated guess can be made as to what their compositions might be. The glass in the interply regions should be rich in B_2O_3, Na_2O and Al_2O_3 because most of the SiO_2 crystallizes out of the original glass. The glass around the Nicalon fibres within the plies can be assumed to have a composition close to that of 7740 borosilicate glass because there seems to be no precipitation of α crystobalite in this area. Another indication that lends credibility to the above assumption is that when the as-received and heat-treated samples were etched in 20% HCl, the glassy phase in the interply region is etched away, whereas

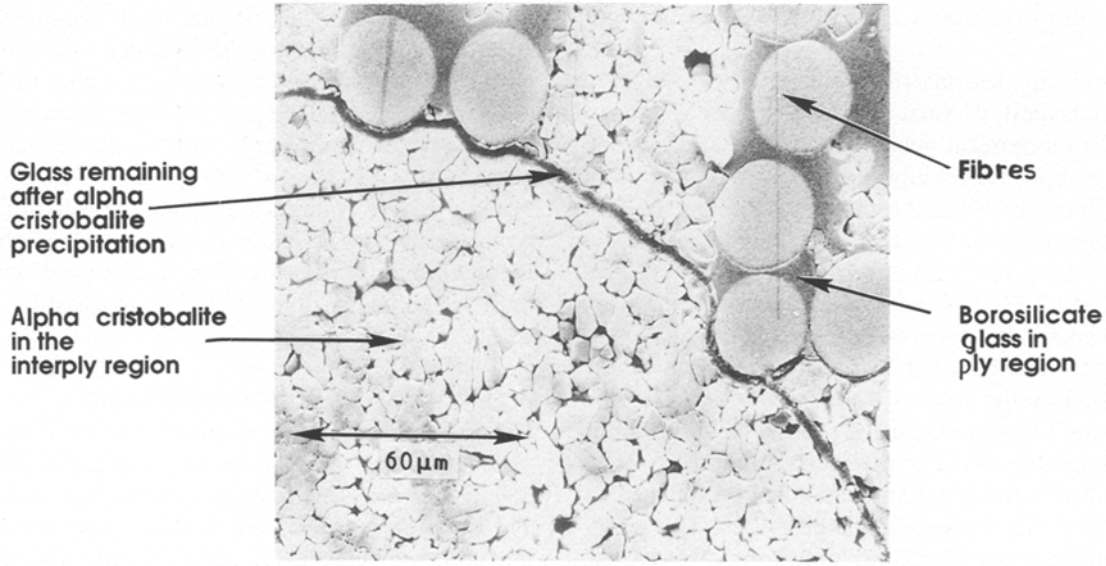

Figure 2 Micrograph showing the difference in structure between the ply and interply regions. (The ply regions consist of borosilicate glass matrix and the interply region consists of alpha cristobalite crystals.)

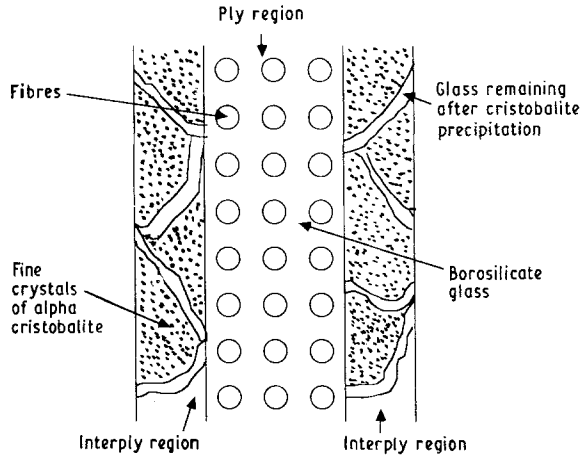

Figure 3 Schematic drawing of the different components present in the different regions of the composite.

the glassy phase within the plies is not etched, implying that it is a more chemically resistant phase, one of the attributes of 7740 borosilicate glass [8, 9].

These observations are consistent with earlier studies on the phase transformations in Pyrex glass. Phase separation in the Pyrex glass system has been widely studied [10–12] and documented. The crystallization of alpha cristobalite out of Pyrex glass has also been observed [13] and the rate of precipitation was found to be a maximum at 1000 °C [14], the hot-pressing temperature of the composite in this study.

4. Experimental procedure

Straight strips of the material were cut off the plate using a diamond blade with a low-speed saw. The dimensions of the samples were as follows: length of 12.7 cm, width of 0.635 cm and thickness of 0.254 cm.

Monotonic tension tests were performed on the unidirectional composite samples fabricated as above, at temperatures ranging from room temperature to 1200 °F (650 °C). The samples were heated indirectly using an induction-heated stainless steel susceptor. At each of these temperatures, samples were tested on a servohydraulic testing machine made by MTS using two different types of grips, one a set of mechanical wedge grips and the other a set of hydraulic grips. Samples tested using wedge grips were tested using stainless steel end tabs which were not used in the case where hydraulic grips were used. All tests were performed under load control and additional tests were performed at 1000 °F (~ 538 °C) and room temperature under stroke control. The strain rate under stroke control was $4 \times 10^{-5} s^{-1}$. The loading rate under load control was 12.4 N s^{-1}. A high-temperature MTS extensometer with alumina rods was used for the measurement of strain.

Several samples were tested at each of the temperatures of testing. The average values of composite tensile strength, composite elastic modulus (stiffness) and the strain to failure from these tests are reported.

5. Composite properties

Fig. 4 shows a plot of the tensile strength of the composite as a function of test temperature. The tensile strength was found to be marginally affected by temperature up to about 425 °C and an abrupt increase at 540 °C and decrease above this temperature. The average value of the tensile strength was found to be 200 MPa at room temperature and 300 MPa at 540 °C. In general, the test results were unaffected by the type of grips used. As shown in Fig. 5, the modulus (stiffness) decreases as the test temperature increases.

The mechanism of final failure is strikingly different as the temperature is increased from room temperature to 540 °C. At the lower temperatures failure occurs by splitting along the length of the sample. The mechanism of failure at 540 °C and above include fibre failure, fibre–matrix debonding and ultimate pull-out of the broken fibres. Macrophotographs of failed samples tested at room temperature and 540 °C are shown in Fig. 6. The strain to failure was found to increase when going from room temperature to 540 °C.

Figs 7 and 8 show the polished (unetched) cross-section of the samples tested at room temperature and 540 °C, respectively. While the fibres do not show any difference due to tensile testing at temperature, the state of the matrix is considerably different depending upon the temperature of testing. In Fig. 7, the matrix

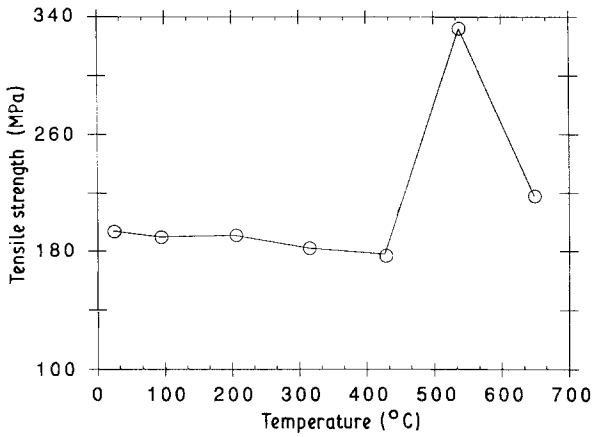

Figure 4 Tensile strength of composite against test temperature.

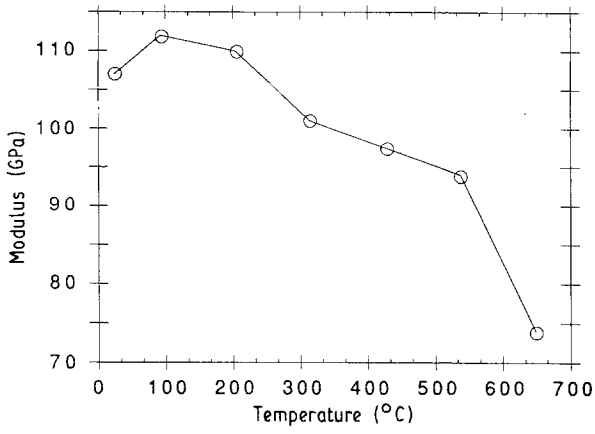

Figure 5 Elastic modulus (stiffness) of composite against test temperature.

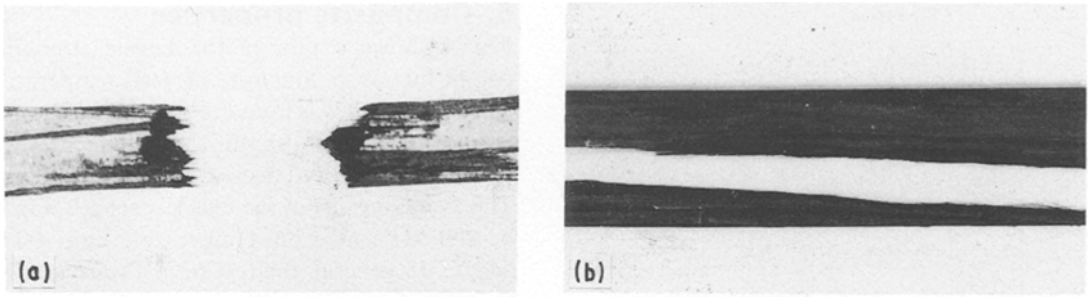

Figure 6 Macrophotographs of failed samples showing (a) longitudinal splitting in a sample tested at room temperature, and (b) fibre failure and pull-out in a sample tested at 540 °C. Magnification × 1.8.

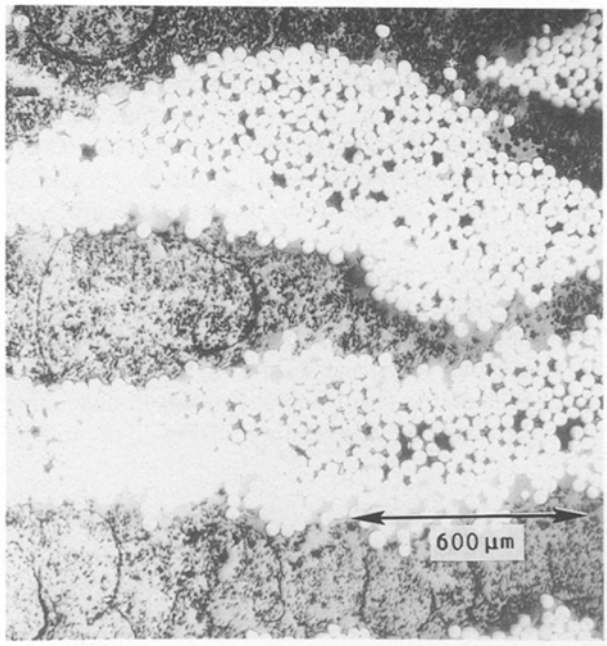

Figure 7 Polished (unetched) cross-section of a sample tested at room temperature showing features that appear to be a very fine distribution of microcracks or voids.

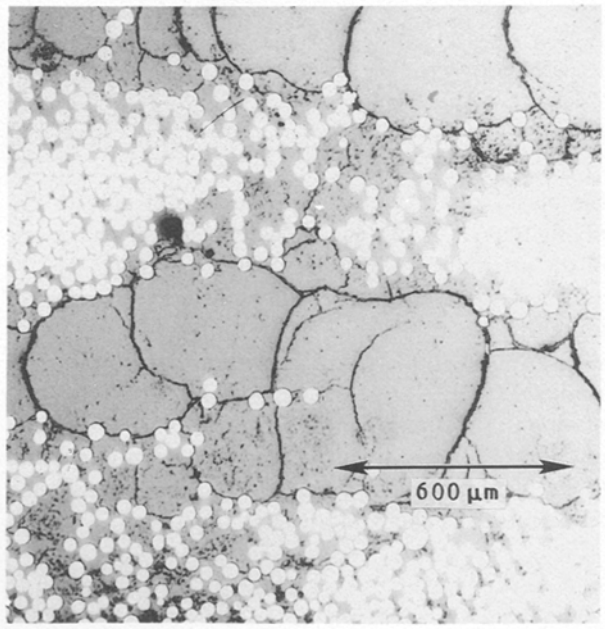

Figure 8 Polished (unetched) cross-section of a sample tested at 540 °C, showing a "cleaner" matrix, compared to Fig. 7.

material in the interply region shows features that appear to be very fine distribution of microcracks or voids. These features were found in all the specimens tested in the temperature range even after repeated polishing of the same section. Fig. 8, on the other hand, shows a "cleaner" matrix or one with a lot fewer cracks/voids for the sample tested at 540 °C.

Any explanation of the behaviour of the composite as a whole is dependent upon the behaviour of the individual constituents. Nicalon has been shown to retain about 90% of its original strength in the 500–550 °C range [15] and thus can be assumed to undergo no major deterioration at the temperatures of testing. Thus the behaviour of the matrix would dictate the behaviour of the composite.

The bulk of the matrix is in the form of crystalline alpha cristobalite. The glassy phase around the alpha cristobalite crystals can be assumed to be rich in B_2O_3, Na_2O and Al_2O_3, the other components of 7740 glass. As discussed earlier, the glassy phase around the fibres should have a composition that is very close to 7740 borosilicate glass. Fig. 9 shows the viscosity versus temperature behaviour [9] for Corning 7740 glass. As shown, the viscosity of glass decreases with increasing temperature. Two main temperatures of interest on this curve are the annealing point and the strain point. The strain point represents the upper limit of serviceability and above the annealing point, distortion of the glass is deemed to occur without any application of stress. The strain point and annealing point of 7740 Borosilicate glass from Fig. 9 can be seen to be 510 and 560 °C, respectively.

The higher strength of the composite at higher temperatures can now be explained. The decreasing viscosity implies an increasing strain capacity of the matrix. This, coupled with a lower yield stress at elevated temperatures, permits more extensive yielding throughout the specimen. A comparison of the microstructures in Figs 7 and 8 appears to show extensive microcracking within the matrix for samples tested at room temperature but not in the sample tested at 540 °C. This would suggest some kind of a crack healing process occurring at this temperature. This would further suggest that at the lower temperature the cracking in the matrix continues to increase until it reaches a level where the matrix fails completely followed by extensive debonding between the

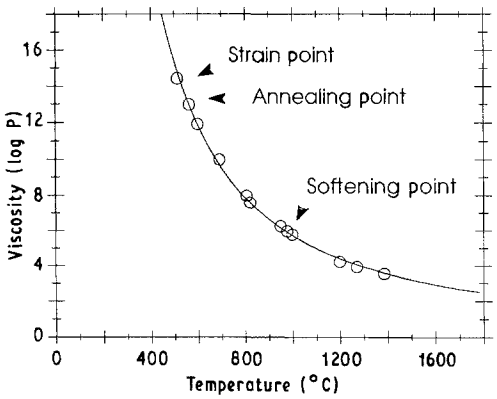

Figure 9 Viscosity versus temperature curve for Corning 7740 borosilicate glass showing the strain point, annealing point, and softening point (from[9]).

fibres and the matrix which manifests itself as longitudinal splitting of the test sample. At 540 °C, on the other hand, the increased plasticity of the matrix allows the fibres to participate in the fracture. After the fibres fail, debonding follows with eventual fibre pull-out. The stiffness and the ultimate strength show reverse trends. The nature of the interface governs the load transfer from the matrix to the fibre which, in turn, governs the stiffness of the composite. The reason for the lower modulus at higher temperatures is thus probably due to the changing nature of the interface. Another contribution to this effect could be due to the decreased contributions of the fibre and the matrix to the composite stiffness at elevated temperature due to some deterioration in properties.

We can now associate the stress–strain response of the material with the different failure mechanisms that are occurring on a microscopic level. Figs 10 and 11 show the stress–strain curves for samples tested at room temperature and 540 °C, respectively. In both these figures, the strain in the curve labelled "extensometer" was obtained using the high-temperature extensometer. In the curve labelled "stroke", the strain was obtained by dividing the displacement between the crossheads by the length of the portion of the specimen between the grips. The latter mentioned curves, even though they include the compliance of the machine, give a more global picture of the damage occurring within the sample as opposed to the stress–strain curves which reflect a one-dimensional response of the material. In Fig. 10, we can see for the room-temperature tested sample, the stress–strain response is linear initially, followed by a non-linear region which includes several drops in the load. The end of the linear region signals the beginning of matrix cracking. The cracks grow in size and number and they connect, which shows up as a load drop in the stress–strain curve. The cracking followed by debonding continues until the load-bearing capacity of the composite is completely lost. For the sample tested at 540 °C, we can see that the stress–strain and the stress–stroke response is linear for a very short portion of the curve. The response for the most part is non-linear reflecting the "plastic" state of the matrix. The ultimate failure of the composite occurs due to failure of the fibre bundles.

It is now obvious [7] that the processing stage plays a crucial role in the final properties obtained for this material. The strength levels obtained for the composite can be further enhanced by eliminating the interply region. This would contribute to the strength of the composite in two ways: by eliminating the alpha cristobalite which does not seem to contribute to the tensile strength of the composite, and by bringing about an increase in the volume fraction of Nicalon fibres which are the main source of the tensile strength of the composite.

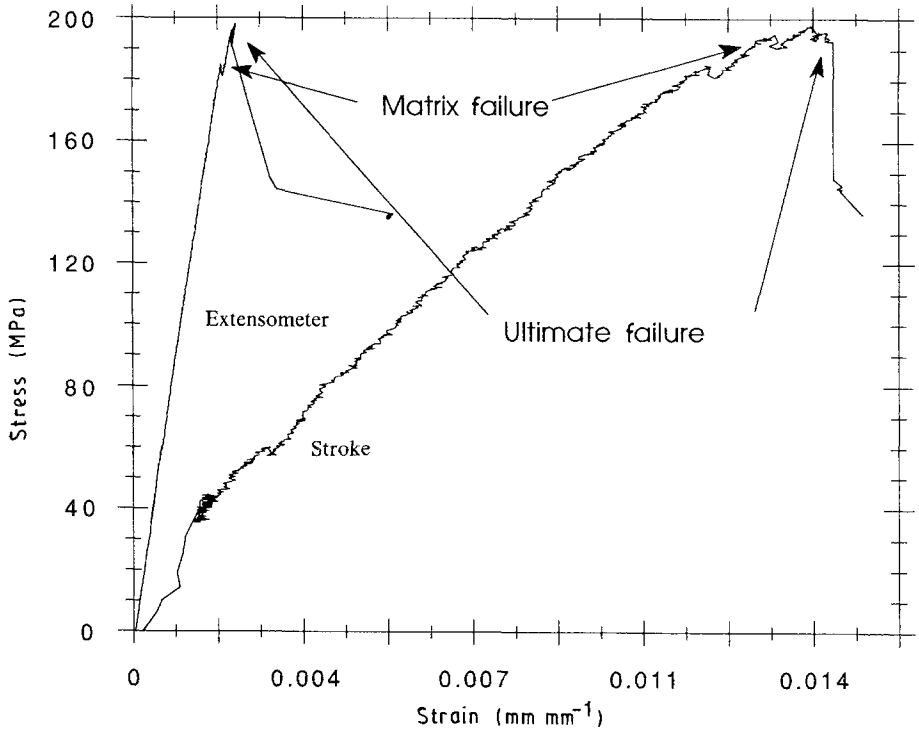

Figure 10 Stress–strain curves for a sample tested at room temperature.

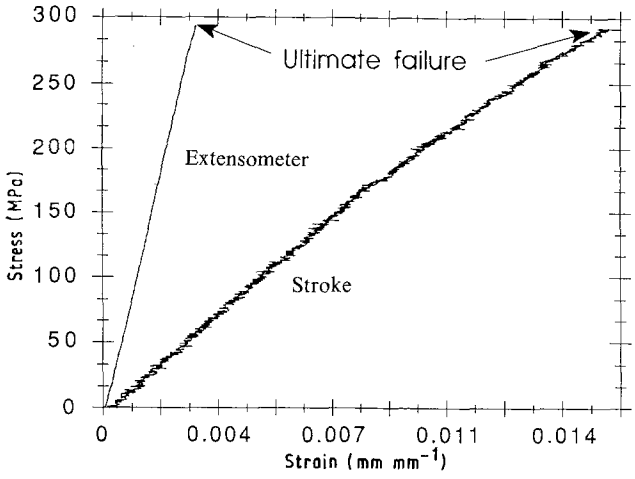

Figure 11 Stress–strain curves for a sample tested at 540 °C.

6. Conclusions

1. The matrix material exists in different forms depending upon the location within the composite. In the interply regions, the bulk of the matrix is in the form of very fine crystals of alpha cristobalite. There are also thick grain-boundary-like features around the alpha cristobalite crystals which appear to be fully glass. The matrix in the ply region appears to be fully glass with a composition close to Corning 7740 borosilicate glass.

2. The tensile strength of the composite remains unaffected by temperature up to about 425 °C and increases dramatically at 540 °C. This increase in strength is associated with the strain point of Corning 7740 borosilicate glass. The modulus of elasticity (stiffness) was found to decrease with increasing temperature.

3. The failure mechanism was found to change from longitudinal splitting of the test sample in the room temperature 425 °C range to that of fibre pull-out at 540 °C and above. Thus, the stress–strain response of the material was associated with matrix cracking and fibre–matrix debonding at lower temperatures while it was associated with fibre failure and pull-out at higher temperatures.

Acknowledgements

The authors acknowledge the help of Mr Larry Davis in conducting some of the mechanical tests, and are grateful for many helpful discussions with the US Air Force's WDRC/MLLN group in general, particularly Mr Larry Zawada and Dr Ted Nicholas.

Reference

1. K. M. PREWO, J. J. BRENNAN and G. K. LAYDEN, *Ceram. Bull.* **65** (1986) 305.
2. K. M. PREWO, *ibid.* **68** (1989) 395.
3. O. SBAIZERO and A. G. EVANS, *J. Amer. Ceram. Soc.* **69** (1986) 481.
4. T. MAH, M. G. MENDIRATTA, A. P. KATZ, R. RAH and K. S. MAZDIYASNI, *ibid.* **68** (1985) C248.
5. K. M. PREWO, B. JOHNSON and S. STARRETT, *J. Mater. Sci.* **24** (1989) 1373.
6. K. M. PREWO and J. J. BRENNAN, *ibid.* **15** (1980) 463.
7. A. BRIGGS and R. W. DAVIDGE, *Mater. Sci. Engng* **A109** (1989) 363.
8. D. C. BOYD and D. A. THOMPSON, "Glass Ceramics", Kirk-Othmer Encyclopedia of Chemical Technology, Vol. 11, 3rd Edn (Wiley, New York, 1980) p. 809.
9. "Properties of Corning's Glass and Glass Ceramic Families", Product information from Corning Glass Works, Corning, NY 14830.
10. R. H. DOREMUS and A. M. TURKALO, *Science* **164** (1969) 418.
11. G. R. SRINIVASAN, I. TWEER, P. B. MACEDO, A. SARKAR and W. HALLER, *J. Non-Cryst. Solids* **6** (1971) 221.
12. W. HALLER, D. H. BLACKBURN, F. E. FLAGSTAFF, and R. J. CHARLES, *J. Amer. Ceram. Soc.* **53** (1970) 34.
13. V. S. R. MURTY and M. H. LEWIS, *J. Mater. Sci. Lett.* **8** (1989) 571.
14. S. M. COX and P. L. KIRBY, *Nature* **159** (1947) 162.
15. "Information about NICALON™ Ceramic Fiber", Product Information from Dow Corning Corporation, Customer Service Department, Midland, MI 48686.

Received 15 January
and accepted 7 June 1991